The possibilistic Kalman filter: definition and comparison with the available methods

A. Ferrero[1], $Fellow, IEEE$, Harsha Vardhana Jetti[2], $Student\ Member$ IEEE,
S. Salicone[1], $SeniorMember, IEEE$

***Abstract*—The Kalman filter is a commonly used algorithm for predicting the state variables of a system. It is based on the model of the system and some measurements (observed over time), which are characterized by their own uncertainty.**

This paper defines a possibilistic Kalman filter, whose main feature is to predict the values of the state variables and the associated uncertainty, also when uncertainty contributions of non-random nature are present. This possibilistic Kalman filter is defined in the mathematical framework of the possibility theory and employes Random-Fuzzy variables and the related mathematics, since these variables can properly represent measurement results together with the associated uncertainty. A comparison with the available methods is provided, as well as a final validation.

***Index Terms*—Measurement Uncertainty; Possibility distributions; Random-Fuzzy Variables; Random contributions; Systematic contributions; Kalman filter.**

I. Introduction

In the last two decades, the possibility theory has been proposed in the literature for the representation and propagation of measurement uncertainty [1]–[6].

Possibility theory represents an effective alternative to the use of probability theory, when both random and systematic contributions to uncertainty are present in the measurement procedure [7]. This is also proved by the various applications available in the literature [8]–[13].

Within this new mathematical framework, measurement results are represented by Random-Fuzzy variables, which are briefly recalled in next Sect. II. Therefore, methods and algorithms aimed at fully exploiting the advantages provided by the Random-Fuzzy variables in expressing measurement uncertainty should be capable of processing them. The Kalman Filter makes no exception and the possibilistic version proposed in this paper, aimed at processing all kinds of uncertainty contributions, is based on these variables.

The Kalman filter (KF) is a well-known algorithm for predicting the state variables of a system [14]. In its classical formulation it represents model uncertainy and measurement uncertainty as normal, unbiased probability distributions [14].

Many different modifications of the KF can be found in the literature to deal with different representations of uncertainty. The Schmidt KF [15] provides an attempt to take into account also systematic uncertainty contributions, as also done with the possibilistic KFs defined in [16] and in this paper. Other contributions can also be found in the literature, to include systematic effects in the Kalman filter, as, for instance [17]–[19]. Both [17] and [18] do not consider explicitly the propagation of the systematic uncertainty contributions, but propose a method to estimate the systematic error affecting the measurement results and compensate for it. On the other hand, [19] proposes to include the systematic error (which is unknown, but bounded) into Bayesian inference and KF. This approach is completely based on probability and appears to be quite complex, since it considers all different possible probability density functions (pdfs) over the given interval, with all possible different mean values.

A few possibilistic KF have also been defined in the literature [20], [21] but, at the Authors' knowledge, all of them consider uncertainty in a sort of semantic way [16], as typical of the fuzzy applications, and not as a well specified concept in metrology, as recommended by [22], [23]. Since uncertainty, in metrology, must be considered according to the definition given by [23], this paper is hence aimed at proposing a possibilistic KF, whose definition is perfectly framed within the present Standards [22], [23].

To validate this proposal, an example is considered, where the velocity of a vehicle, along with its associated measurement uncertainty, has to be estimated, with a Kalman filter. This example is described in Sect. III.

Five different approaches to the KF are applied and compared with each other: two probabilistic approaches (the classical KF and the Schmidt KF [15]), two possibilistic approaches (the possibilistic Kalman filter proposed in [16] and a refinement of it, proposed in this paper) and a hybrid KF, which combines the classical KF and the possibilistic KF defined in this paper, for the random and systematic uncertainty contributions respectively.

This last version has been considered, as shown in Sect. IV, to validate the proposed possibilistic KF by processing the systematic and random contributions to uncertainty separately, according to their natural mathematical representation [2], [3]. Under these conditions, the highest accuracy is achieved, as shown in Sect. IV, at the cost of a higher computational burden that, at present, makes the hybrid KF suitable only as a reference method.

The five approaches will be compared, in the following, both from the theoretical point of view and with the considered simple example. Since the classical KF and the Schmidt KF have been already proposed in the literature since long ago,

The authors are with: [1]Politecnico di Milano, Department of Electronics, Information and Bioengineering, P.za Leonardo da Vinci 32, 20133 Milano, Italy (e-mail: alessandro.ferrero@polimi.it, simona.salicone@polimi.it); [2]Politecnico di Milano, Department of Energy, Via Lambruschini 4, 20156 Milano, Italy (e-mail: harshavardhana.jetti@polimi.it)

and the possibilistic Kalman filter has been already experimentally validated in [16], all comparisons in this paper will be based on simulated data, in order to ensure homogeneous conditions.

II. A SHORT MATHEMATICAL REVIEW

This section recalls the Random-Fuzzy variables (RFVs) very briefly, since they will be used in the following. For more details, the Readers are addressed to the available numerous contributions in the literature.

Since an RFV is defined by two possibility distributions (PDs), it is necessary to first recall a PD. A possibility distribution $r(x)$ is a function:

$$r(x) : \Re \rightarrow [0, 1]$$

where

$$\max r(x) = 1$$

which represents the normalization condition. In other words, the maximum value of a PD is always 1, as can be seen in the examples in Fig. 1. Furthermore, if one considers the cuts of the PD at given levels α (with $0 \leq \alpha \leq 1$), closed intervals are obtained, denoted by α-cuts. As an example, the pink lines in Fig. 1 show the α-cuts of the PDs at level $\alpha = 0.2$.

From the same figure, it can be also noted that, except for the rectangular PD in the upper plot (for which the α-cuts are all equal to each other for every level α), as the α value decreases, the corresponding α-cut becomes wider. In particular, the α-cut at level α^* contains all α-cuts for levels $\alpha > \alpha^*$. From the mathematical point of view, it can be stated that the α-cuts are nested intervals[1]. [1], [24]. Furthermore, from the metrological point of view, a PD can be considered a mathematical representation of a measurement result and every α-cut can be assimilated to a coverage interval with coverage probability $1 - \alpha$ [1].

To represent a measurement result, a PD should be built from the available metrological information [2], [25]. For example, the rectangular PD shown in Fig. 1 (a) is generally employed to represent *total ignorance* [1], [24], [26] which means that we know that the measured value falls in the given interval ($[4.9\ 5.1]$ for the given figure) but we do not know where and we do not have any other additional information about this distribution.

On the other hand, when some additional information is available, this should be properly used to build the PD. In many practical cases, it may happen, for instance, that it is known how the measurement results distribute over the given interval, i.e. a pdf is given. In this situation, the PD can be obtained from the given pdf by applying a suitable probability-possibility transformation [1], [24], [26], [27], which mantains the same coverage intervals at the same coverage probability. As an example, plots (b), (c) and (d) in Fig. 1 show the PDs built, respectively, from a uniform pdf, a normal pdf and a triangular pdf.

Possibility distributions can be combined according to many different fuzzy operators [1]. Therefore, by choosing the proper fuzzy operator in combining two PDs (i.e the min t-norm), it is possible to mathematically model the combination of measurement results which physically combine in a systematic way [1], [2]. On the other hand, by choosing other fuzzy operators (i.e. the $Frank$ t-norm or the $Dombi$ t-norm), it is

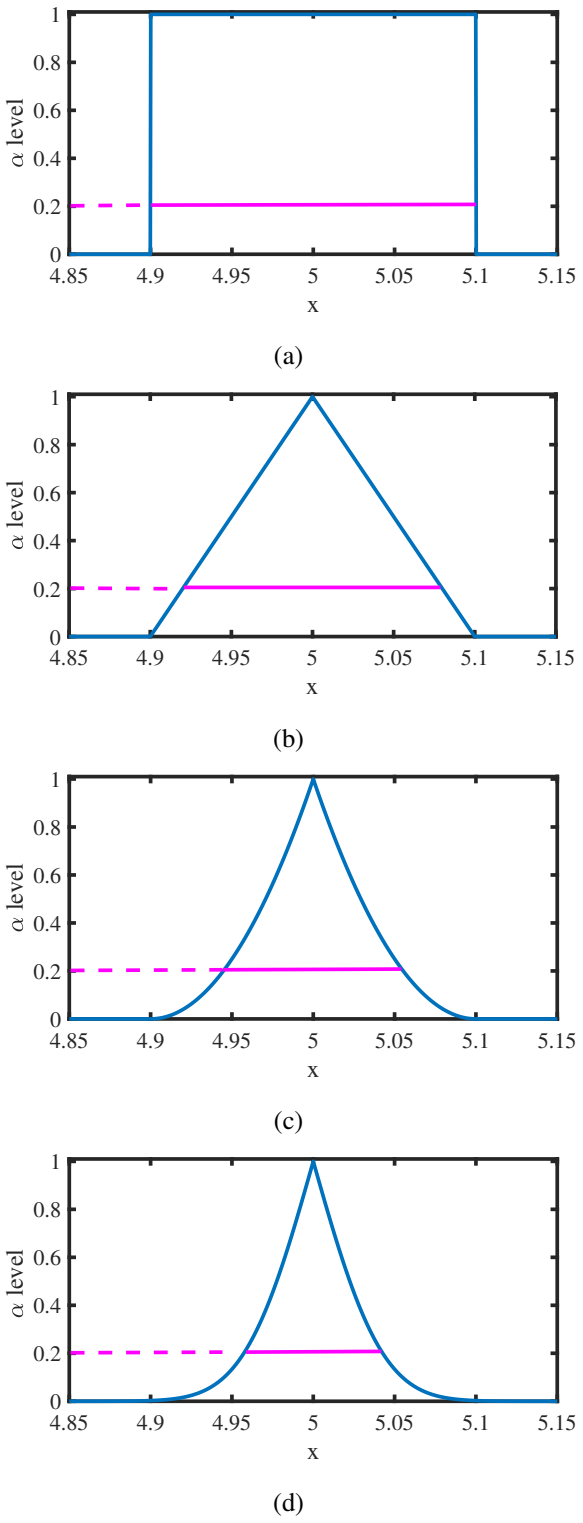

Fig. 1. Example of PDs defined over interval $[4.9, 5.1]$ and confidence intervals at a specific level α.

[1]Because of this property, the PDs can be dealt within the mathematical possibility theory [1]

possible to approximate the combination of two measurement results which physically combine in a random way [1].

The same measurement result however can be affected by both random and systematic contributions to uncertainty. In order to distinguish them and propagate them correctly, fuzzy variables of type 2 should be used, in particular the Random-Fuzzy variables [1], [7], [26], as shown in Fig. 2.

An RFV is made of two PDs, an internal and an external one, so that it can represent a measurement result affected by both random and systematic contributions to uncertainty [1]. In particular, the systematic contributions are included in the *internal PD* (green line in Fig. 2), while the random contributions are included in one *random PD* that, when combined with the internal PD, provides the *external PD* (pink line in Fig. 2).

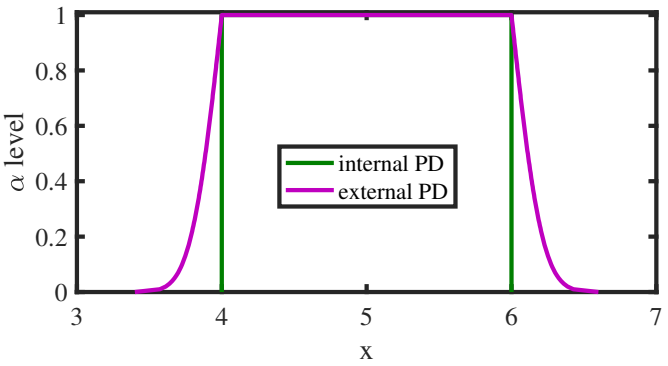

Fig. 2. Example of RFV.

III. The Considered Example

A simple example is considered, in which a vehicle is moving at a velocity $v_{\mathrm{ref}}(t)$, according to the impressed acceleration $a_{\mathrm{ref}}(t)$, as shown in Fig. 3.

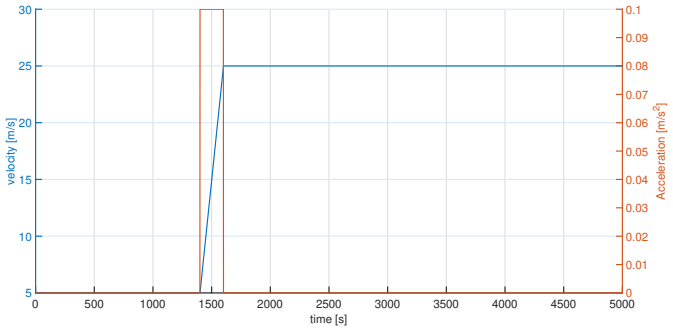

Fig. 3. Reference values of velocity (blue line) and acceleration (red line) over time.

A Kalman filter is used to estimate velocity and acceleration of the vehicle.

Eq. (1) shows the state equations of the model:

- v_k and a_k are velocity and acceleration of the vehicle at time k;
- w_k^v and w_k^a are the standard deviation of the noise in velocity and acceleration respectively at time k;
- τ is the time period within two successive measurements

$$\begin{aligned} v_k &= v_{k-1} + \tau \cdot a_{k-1} + w_k^v \\ a_k &= a_{k-1} + w_k^a \end{aligned} \tag{1}$$

Fig. 4 shows the alternation of the prediction and assimilation steps in the classical KF.

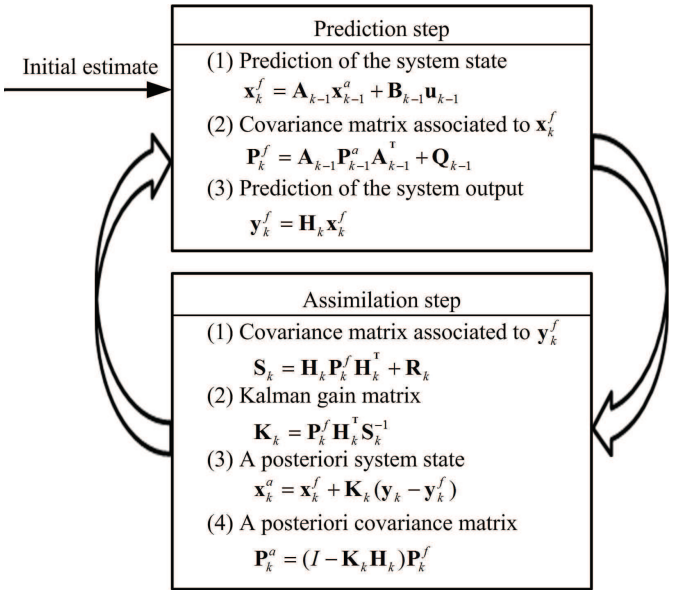

Fig. 4. Prediction and assimilation steps alternation in the classical Kalman filter.

For the considered example, the state vector is $\mathbf{x}_k = \begin{bmatrix} v_k \\ a_k \end{bmatrix}$; the *state-transition matrix*, denoted with $\mathbf{A}_{k-1}$ in Fig. 4, is constant $\mathbf{A}_k = \mathbf{A} = \begin{bmatrix} 1 & \tau \\ 0 & 1 \end{bmatrix}$; the *control-input matrix*, denoted with $\mathbf{B}_k$ in Fig. 4 is zero; the *transformation matrix*, denoted with $\mathbf{H}_k$ in Fig. 4, is: $\mathbf{H}_k = \mathbf{H} = \begin{bmatrix} 1 & 0 \\ 0 & 1 \end{bmatrix}$ and the measurement vector is: $\mathbf{y}_k = \begin{bmatrix} v_{mk} \\ a_{mk} \end{bmatrix}$.

As shown in Fig. 4, two matrices have to be defined: the covariance matrix $\mathbf{Q}_k$, which considers the process noise, and the covariance matrix $\mathbf{R}_k$, which considers the measurement noise, that is the uncertainty associated to the measured values. Therefore, it is: $\mathbf{Q}_k = \begin{bmatrix} w_{k\,v}^2 & 0 \\ 0 & w_{k\,a}^2 \end{bmatrix}$ and $\mathbf{R}_k = \begin{bmatrix} u_{k\,v}^2 & 0 \\ 0 & u_{k\,a}^2 \end{bmatrix}$, where $u_{k\,v}$ is the standard uncertainty associated to the measured values of velocity and $u_{k\,a}$ is the standard uncertainty associated to the measured values of acceleration.

The following assumptions are done, as far as the initial values of the state variables and their associated uncertainty values are considered.

- It is supposed that $\mathbf{Q}_k$ and $\mathbf{R}_k$ do not vary with k, i. e. $\mathbf{Q}_k = \mathbf{Q} = \begin{bmatrix} w_v^2 & 0 \\ 0 & w_a^2 \end{bmatrix}$ and $\mathbf{R}_k = \mathbf{R} = \begin{bmatrix} u_v^2 & 0 \\ 0 & u_a^2 \end{bmatrix}$.
- The initial velocity of the vehicle is assumed to be a normal distribution with mean equal to the first measured value of velocity (v_{m1}) and standard deviation $0.003\,\mathrm{m/s}$. Therefore: $v_0 = v_{m1}$ m/s and $w_v = 0.003$ m/s. This last value has been chosen by considering the accuracy

of a GPS, which is quite accurate compared to the speedometer of the vehicle, and it is directly retrieved from the official GPS website [28].
- The initial acceleration is assumed to be a normal distribution centered at the first measured value of acceleration (a_{m1}) obtained from the accelerometer, with a standard deviation of $0.0005\ m/s^2$, due to some kind of noise either due to the circuit or due to the driver applying force on the accelerator. Therefore: $a_0 = a_{m1}\ \mathrm{m/s^2}$ and $w_a = 0.0005\ \mathrm{m/s^2}$.

On the other side, at every step k, as far as measurements are concerned, the uncertainty contributions affecting the measured values must be also considered. It has been assumed that the measured values are affected by both random and systematic uncertainty contributions. In particular, as far as the velocity is concerned, typical accuracy values have been assumed for the on-board sensor, which are generally one or two orders of magnitude less accurate than a GPS-based speedometer:

- The random contribution is supposed to be normally distributed, with a standard deviation $u^v_{\mathrm{ran}} = 0.16\ \mathrm{m/s}$.
- A systematic error is also supposed to be present, with an estimated value $e^v_{sys} = 0.3\ \mathrm{m/s}$. But this value is supposed to be unknown, so that a systematic contribution is modeled, laying in the interval $\pm b_{\mathrm{sys}} = \pm 0.32\ \mathrm{m/s}$ (which include the true systematic error e^v_{sys}).

On the other hand, as far as the acceleration is concerned, it is supposed that no systematic contributions affect the measurement procedure, while a typical random contribution is considered which is supposed to be normally distributed, with a standard deviation $u^a_{\mathrm{ran}} = 0.005\,\mathrm{m/s^2}$ that is one order of magnitude less accurate than the model.

For the Kalman filter algorithm, five different methods are exploited in this paper, in order to show a comparison between the different obtained results and to draw some conclusions about the performance of the different methods. Sect. III-A shows the results provided by the classical Kalman filter (KF) and Sect.III-B shows the results provided by the Schmidt KF, both of which are defined on a probability framework. On the other hand, Secs. III-C and III-D show the results provided by possibilistic KFs: the possibilistic KF defined in [16] is applied in Sect. III-C, while a refinement of it is considered in Sect. III-D. In Sect. IV, the obtained results are compared with those provided by an hybrid KF, employed to validate the results provided by the possibilistic KF, as anticipated in the Introduction.

A. Classical Kalman filter

In the first simulation, the classical Kalman filter, as shown in Fig. 4, is applied, where, according to the above assumptions (Sect. III), at $k = 0$ it is:

- $\mathbf{x}^a_0 = \begin{bmatrix} v_{m1} \\ a_{m1} \end{bmatrix}$;
- $\mathbf{P}^a_0 = \mathbf{Q}$.

As far as the measurements are concerned, the value of the measured velocity v_k is simulated, at every step k, as a random extraction from a normal distribution with mean value $v_{\mathrm{ref}}(k) + e^v_{sys}$ and standard deviation u^v_{ran}. The standard uncertainty value associated to the measured value v_k is u_v, which must take into account for both random and systematic uncertainty contributions. As suggested by the GUM [22]:

$$u_v = \sqrt{\left(u^v_{\mathrm{ran}}\right)^2 + \left(u^v_{\mathrm{sys}}\right)^2}$$

where u^v_{sys} is the standard deviation of the pdf associated to the considered systematic contribution. When the GUM [22] is followed and probability theory is employed for uncertainty evaluation, it is a common practice to assign a uniform distribution over the interval of possible variation of the systematic contribution. Under this assumption, it is: $u^v_{\mathrm{sys}} = \frac{b_{\mathrm{sys}}}{\sqrt{3}}\ \mathrm{m/s}$.

Similarly, the simulated measured acceleration a_k at every step k is a random extraction from a normal distribution with mean value $a_{\mathrm{ref}}(k)$ and standard deviation u^a_{ran}. Since only random contributions are supposed to affect the acceleration measurement procedure, the standard deviation associated to a_k is u^a_{ran}.

At every step, the prediction of the state vector is obtained (Eq. (1) in the upper part of Fig. 4) and the covariance matrix associated to the state vector is evaluated (Eq. (2) in the upper part of Fig. 4). This covariance matrix has a crucial role in the evaluation of the *gain matrix* $\mathbf{K}_k$ (Eqs. (1) and (2) in the lower box of Fig. 4), which is then used to evaluate the *a posteriori* value of the state vector (Eq. (3) in the lower box of Fig. 4).

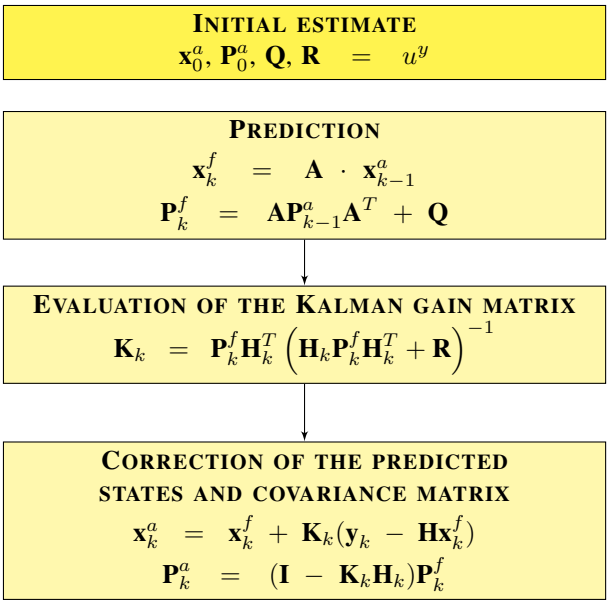

Fig. 5. Classical Kalman filter algorithm.

The applied algorithm for the classical KF is therefore summarized in Fig. 5, while the results of the simulation are reported in Fig. 6 and 7.

The blue line in Fig. 6 represents the difference between the predicted velocity and v_{ref}. This difference is of course not constant but, after a transition of about 250 iterations (i. e. 250 s, since one iteration is done every 1 s) oscillates around the value e_{sys}, as expected, because of the presence of the systematic error in the measurements. On the other hand, the red lines represent the evaluated uncertainty interval.

In particular, for each iteration k, the provided interval is the $\pm 3\sigma_k$ interval [22], where σ_k is the standard uncertainty associated to the *a posteriori* value of the velocity at step k, that can be retrieved from the values in the main diagonal of matrix $\mathbf{P}_k^a$. It can be clearly seen that the difference between the predicted velocity and $v_{\mathrm{ref}}(t)$ is always outside the obtained uncertainty bounds. So, even if the classical Kalman filter can predict quite well the velocity of the vehicle (at steady state), it can be concluded that it underestimates the measurement uncertainty and therefore it is not suitable when also systematic contributions to uncertainty are present. Furthermore, the convergence time is quite high.

Fig. 7 shows the results obtained for the acceleration and the blue and red lines have the same meaning as in Fig. 6. In this case, since only random contributions affect the measured values, the $\pm 3\sigma$ uncertainty intervals contain the measured values except, of course, when the acceleration has a sudden variation.

B. Schmidt Kalman filter

The Schmidt Kalman filter has been proposed in [15], as a variation of the classical KF, to consider also the systematic uncertainty contributions. The Schmidt Kalman algorithm is summarized in Fig. 8.

It considers the systematic contribution as an additional state variable. So, the systematic contributions are modeled as a separate matrix of states and the corresponding noise covariance matrix. Therefore, new matrices, in addition to the ones defined in the classical KF have to be defined for modeling the systematic contribution:

- $\mathbf{H}_{\mathrm{B}} = \begin{bmatrix} 1 \\ 0 \end{bmatrix}$
- $B = {u_{\mathrm{sys}}^v}^2 = 0.32^2/3$
- $\mathbf{D}_0^a = \begin{bmatrix} 0 \\ 0 \end{bmatrix}$

where B is the variance of the systematic contribution and $\mathbf{D}$ is the cross covariance matrix between the random and systematic errors. It is a zero matrix because the systematic and random errors are independent in the considered example. The Readers are addressed to [15] for further details.

The initial values of $\mathbf{x}_0^a$, $\mathbf{Q}$ and $\mathbf{P}_0^a$ are the same as in Sect. III-A.

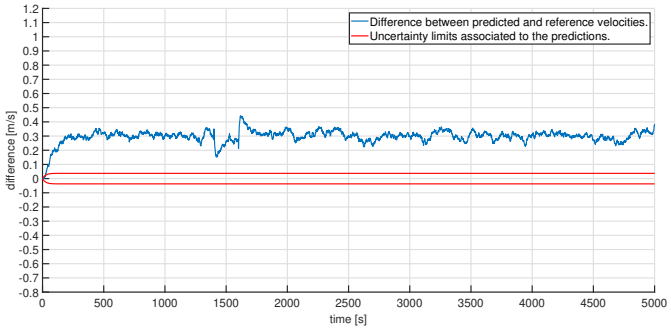

Fig. 6. Difference in the reference and predicted velocity values (blue line) provided by the classical Kalman filter, together with the predicted uncertainty interval (red lines).

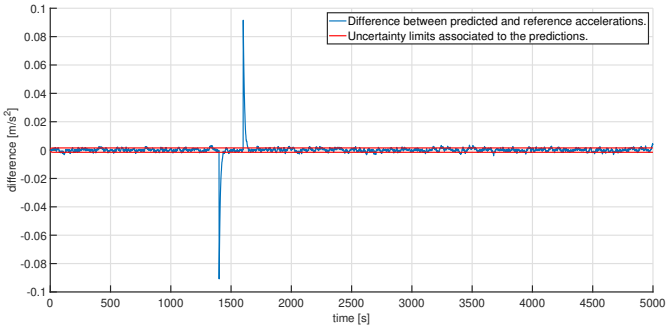

Fig. 7. Difference in the reference and predicted acceleration values (blue line) provided by the classical Kalman filter, together with the predicted uncertainty interval (red lines).

INITIAL ESTIMATE

$$\mathbf{x}_0^a,\ \mathbf{P}_0^a,\ \mathbf{Q},\ \mathbf{R},\ \mathbf{D}_0^a,\ \mathrm{B}$$

PREDICTION

$$\mathbf{x}_k^f = \mathbf{A} \cdot \mathbf{x}_{k-1}^a$$
$$\mathbf{P}_k^f = \mathbf{A}\mathbf{P}_{k-1}^a\mathbf{A}^T + \mathbf{Q}$$
$$\mathbf{D}_k^f = \mathbf{A} \cdot \mathbf{D}_{k-1}^a$$

EVALUATION OF THE KALMAN GAIN MATRIX

$$\mathbf{K}_k = (\mathbf{P}_k^f\mathbf{H}_k^T + \mathbf{D}_k^f\mathbf{H}_{\mathrm{B}}^T)(\mathbf{H}_k\mathbf{P}_k^f\mathbf{H}_k^T + \mathbf{H}_{\mathrm{B}}\mathbf{D}_k^{fT}\mathbf{H}_k^T + \mathbf{H}_k\mathbf{D}_k^f\mathbf{H}_b^T + \mathbf{H}_{\mathrm{B}}B\mathbf{H}_{\mathrm{B}}^T + \mathbf{R})^{-1}$$

CORRECTION OF THE PREDICTED STATES AND COVARIANCE MATRIX

$$\mathbf{x}_k^a = \mathbf{x}_k^f + \mathbf{K}_k(\mathbf{y}_k - \mathbf{H}\mathbf{x}_k^f)$$
$$\mathbf{P}_k^a = (\mathbf{I} - \mathbf{K}_k\mathbf{H}_k)\mathbf{P}_k^f - \mathbf{K}_k\mathbf{H}_{\mathrm{B}}\mathbf{D}_k^{fT}$$
$$\mathbf{D}_k^a = \mathbf{D}_k^f - \mathbf{K}_k(\mathbf{H}_k\mathbf{D}_k^f + \mathbf{H}_{\mathrm{B}}B)$$

Fig. 8. Schmidt Kalman filter algorithm.

Also the simulated measured values v_k of velocity are obtained as in Sect. III-A but, in this case, the associated standard uncertainty value is u_{ran}^v, because in the Schmidt Kalman filter, the systematic uncertainty is propagated as a separate matrix.

The simulated measured values of acceleration a_k and the associated standard deviation are also obtained as in Sect. III-A.

The results of the simulations are reported in Fig. 9 and 10, where the blue and the red lines have the same meaning as in Figs. 6 and 7.

The results obtained for the acceleration are pretty much the same as in the previous case in Sect. III-A, while a difference can be seen in the velocity.

The Schmidt Kalman filter is aimed at considering systematic uncertainty contributions and indeed the uncertainty intervals are significantly larger than those obtained in Sect. III-A, but they do not yet contain the actual velocity of the vehicle. Therefore, even if the Scmidt KF provides a better

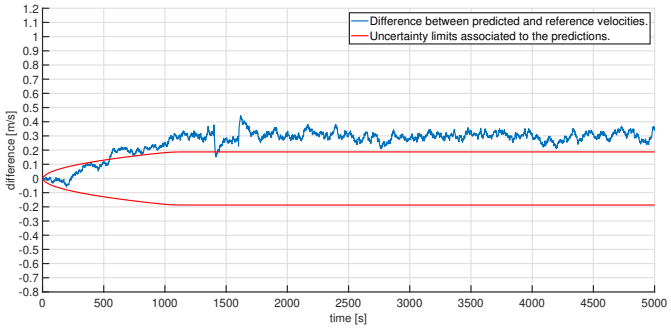

Fig. 9. Difference in the reference and predicted velocity values (blue line) provided by the Schmidt Kalman filter, together with the predicted uncertainty interval (red lines).

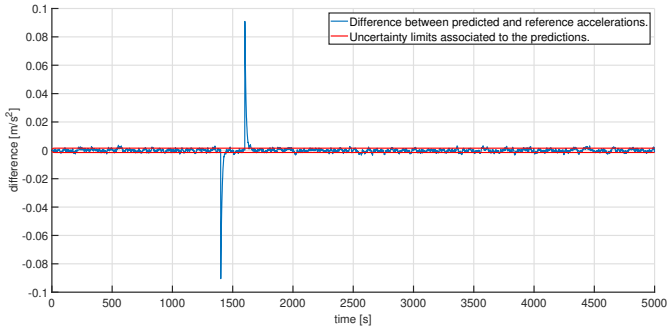

Fig. 10. Difference in the reference and predicted acceleration values (blue line) provided by the Schmidt Kalman filter, together with the predicted uncertainty interval (red lines).

estimation of the measurement uncertainty in the presence of systematic contributions than the classical KF, uncertainty is still underestimated.

C. The possibilistic Kalman filter

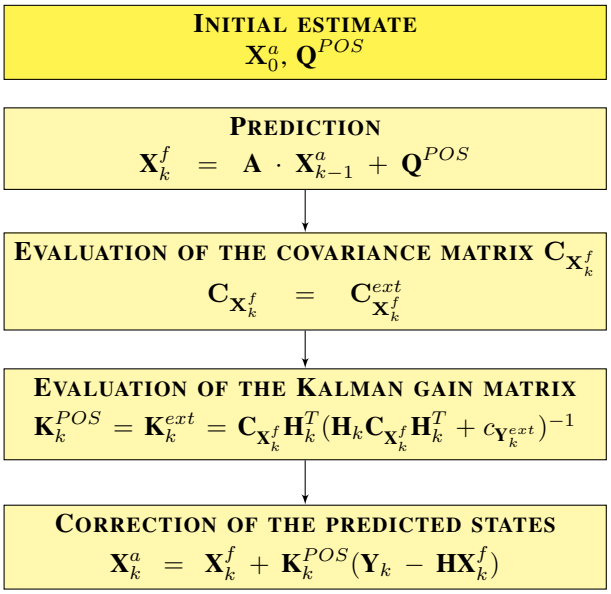

Fig. 11. Possibilistic Kalman filter algorithm defined in [16].

This section considers the application of the possibilistic Kalman filter defined in [16], with the aim to consider also the presence of systematic contributions to uncertainty.

The basic equations of this algorithm defined in [16] are given in Fig. 11[2]. All variables in the state vectors are RFVs and the iterations are performed using RFV mathematics [1], [2], [29], so that both random and systematic contributions can be mathematically represented and combined according to their different nature [1], [2]. Furthermore:

- as for the matrix which considers the model uncertainties (matrix $\mathbf{Q}$ in the classical Kalman filter), according to the assumptions reported in Sect. III, we define a vector of RFVs $\mathbf{Q}^{POS}$ where:
  - the element related to velocity is an RFV in which there is no internal PD and the random PD is obtained by transforming [1] a zero mean normal pdf with standard deviation w^v in the possibility domain;
  - the element related to acceleration is an RFV in which there is no internal PD and the random PD is obtained by transforming [1] a zero mean normal pdf with standard deviation w^a in the possibility domain;
- as for the initial state vector $\mathbf{X}_0^a$, it is assumed that
  - the initial velocity is an RFV in which there is no internal PD and the random PD is obtained by transforming [1] a normal pdf with mean equal to the first measured value for velocity (v_{m1}) and standard deviation w^v in the possibility domain;
  - the initial acceleration is an RFV in which there is no internal PD and the random PD is obtained by transforming [1] a normal pdf with mean equal to the first measured value for acceleration (a_{m1}) and standard deviation w^a in the possibility domain;
- as for the measured values, for every step k, the RFV associated to the simulated measured velocity is centered on v_k (obtained as in Sect. III-A) and
  - the internal PD is a rectangular PD with width $\pm b_{sys}$ around v_k;
  - the random PD is obtained by transforming [1] a zero mean normal pdf, with standard deviation u_{ran}^v in the possibility domain.

  On the other hand, the RFV associated to the simulated measured acceleration is centered on a_k (obtained as in Sect. III-A) and:
  - the internal PD is nil;
  - the random PD is obtained by transforming [1] a normal pdf, with mean a_k and standard deviation u_{ran}^a in the possibility domain.

The obtained results are shown in Figs. 12 and 13. In the possibilistic approach, the difference between the predicted velocity/acceleration and the corresponding reference values are RFVs[3]. Therefore, the blue lines in Fig. 12 and 13 represent the mean values of these RFVs. On the other hand, the red lines represent, for every iteration k, the width of the α-cut at level $\alpha = 0.01$ of the predicted velocity/acceleration respectively, i. e. the confidence level at coverage probability

[2]The Readers are addressed to [16] for more details.
[3]Since the predicted velocity and acceleration are RFVs.

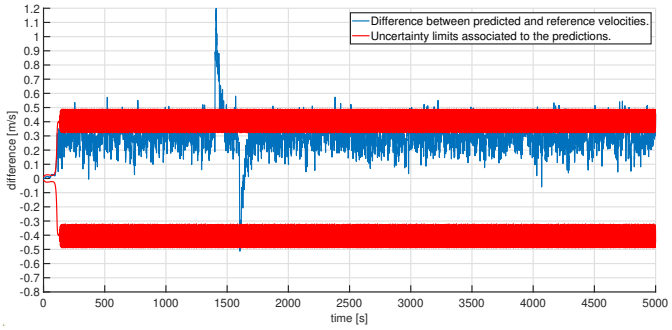

Fig. 12. Difference in the reference and predicted velocity values (blue line) provided by the possibilistic Kalman filter defined in [16], together with the predicted uncertainty interval (red lines).

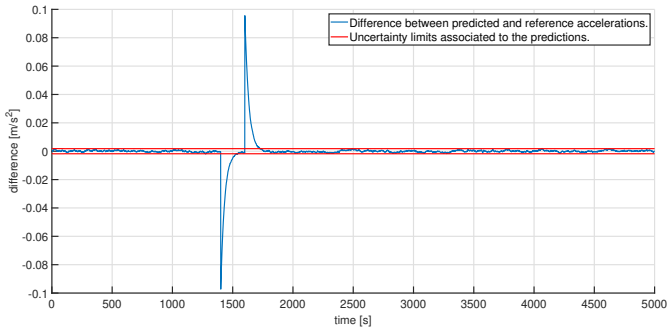

Fig. 13. Difference in the reference and predicted acceleration values (blue line) provided by the possibilistic Kalman filter defined in [16], together with the predicted uncertainty interval (red lines).

99%.

With respect to the results provided by the classical KF and Schmidt KF, which both underestimate the measurement uncertainty, the possibilistic KF is able to consider correctly also the systematic contribution, so that the provided confidence intervals always include the systematic error e_{sys}. Furthermore, the time of convergence of the possibilistic KF is 117 iterations.

However, Fig. 12 also shows a problem in the obtained results, i.e. the non-negligible oscillations. In fact, if, after reaching convergence, the standard deviation of the results shown in the blue line is evaluated, a value of $88.2 \cdot 10^{-3}\,\mathrm{m/s}$ is obtained, which is much higher than the value obtained when the results of the classical KF ($29.9 \cdot 10^{-3}\,\mathrm{m/s}$) and the Schmidt KF ($26.7 \cdot 10^{-3}\,\mathrm{m/s}$) are considered.

This result is not desirable, since the aim of a KF is a good prediction of both the state variable and its uncertainty. However, in this case, the prediction of the uncertainty values is not satisfactory. The reason for these oscillations can be attributed to the very high values taken by the gain matrix $\mathbf{K}_k^{POS}$.

As also summarized in Fig. 11, the gain matrix is evaluated according to the covariance matrix $\mathbf{C}_{\mathbf{X}_k^f}$. In [16], it has been suggested that the covariance matrix is evaluated according to the external membership function of the RFVs, so that the overall uncertainty is taken into account. Therefore, under this assumption: $\mathbf{C}_{\mathbf{X}_k^f} = \mathbf{C}_{\mathbf{X}_k^f}^{ext}$ and $\mathbf{K}_k^{POS} = \mathbf{K}_k^{ext}$ [16] (see again Fig. 11).

D. A new definition for the possibilistic Kalman filter

In the previous Sect. III-C, it has been shown how the possibilistic KF is able to correctly evaluate the measurement uncertainty due to both random and systematic contributions, but it is not as efficient in predicting the velocity values, as proved by the oscillations in the blue line in Fig. 12. In this section, a modified possibilistic KF is defined, in order to maintain the advantages of the already defined possibilistic KF but also to improve the state variable prediction.

As stated in previous Sect. III-C, the oscillations in the blue line in Fig. 12 are due to the very high values in the gain matrix $\mathbf{K}_k^{POS}$, which is evaluated according to the possibilistic covariance matrix $\mathbf{C}_{\mathbf{X}_k^f} = \mathbf{C}_{\mathbf{X}_k^f}^{ext}$.

Since the covariance matrix is evaluated starting from the external PDs of the RFVs representing the state variables, its elements are quite high. In this paper, we propose to evaluate the possibilistic Kalman gain matrix, according to the possibilistic covariance matrix $\mathbf{C}_{\mathbf{X}_k^f} = \mathbf{C}_{\mathbf{X}_k^f}^{ran}$. This means that the possibilistic variances and covariances are evaluated from the random PDs of the RFVs of the state variables. Similarly, also the possibilistic variance of measurements $\mathbf{Y}_k$ is evaluated for its random PD $\mathbf{Y}_k^{ran}$. In this way, since the possibilistic variance and covariance decrease, also the elements in the Kalman gain matrix decrease.

This choice is motivated by the fact that the Kalman gain matrix requires only the evaluation of the amount of variation about the measured value, and not the amount of deviation with respect to the expected value. Since the amount of variation about the measured value is indeed given by the random contributions, and not by the systematic ones, the choice of considering only the random PDs instead of the external PDs in the evaluation of the possibilistic variances and covariances appears to be justified.

Under this new assumption, the algorithm for the possibilistic Kalman filter is schematically represented in Fig. 14. With respect to the algorithm in Fig. 11, the different evaluation of the covariance matrix can be readily perceived and, consequently, the different Kalman gain matrix can be also seen.

There is also another difference between the two algorithms in Figs. 11 and 14, shown in the last equation. In the new definition, the correction of the state variables is done by considering, in the given equation, only the internal PD of the RFV associated to the measurement value. This is more coherent with the classical KF, in which the correction of the state variables only depends on the value v_k of the measured velocity and not on its uncertainty. In the same way, by processing $\mathbf{Y}_k^{int}$, all possible values of the measured velocity caused by the presence of a systematic error are taken into account, but the random variability about this value is not considered in the state prediction.

The obtained results are shown in Figs. 15 and 16, where the red and blue lines have the same meaning as in Figs. 12 and 13. Fig. 15 clearly shows that the oscillations reported in Fig. 12 have been completely eliminated. Convergence is obtained after about 153 iterations, so convergence is slower than with the original possibilistic Kalman filter, but the results are

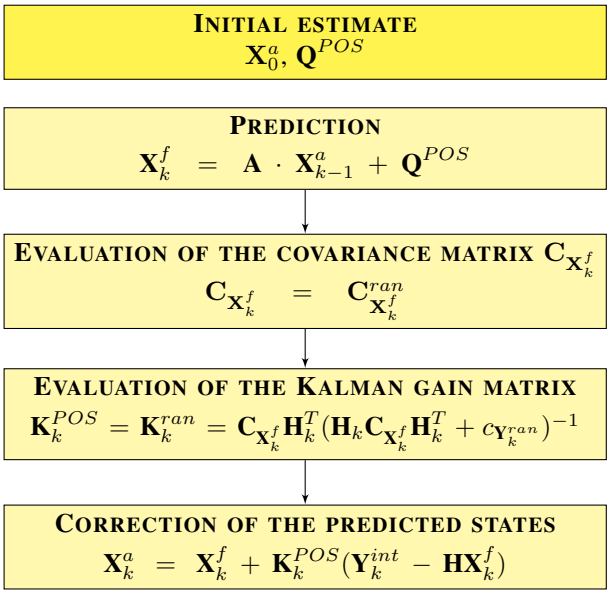

Fig. 14. The defined possibilistic Kalman filter algorithm.

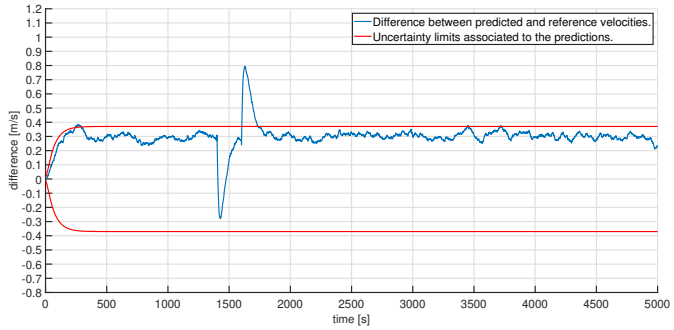

Fig. 15. Difference in the reference and predicted velocity values (blue line) provided by the possibilistic Kalman filter defined in this paper, together with the predicted uncertainty interval (red lines).

really improved. If, after reaching convergence, we evaluate the standard deviation of the results in the blue line, we obtain a value of $22.4 \cdot 10^{-3}\,\mathrm{m/s}$, which is lower than in all previous cases.

The good estimation of uncertainty is also confirmed, since the predicted values of velocity are well inside the predicted

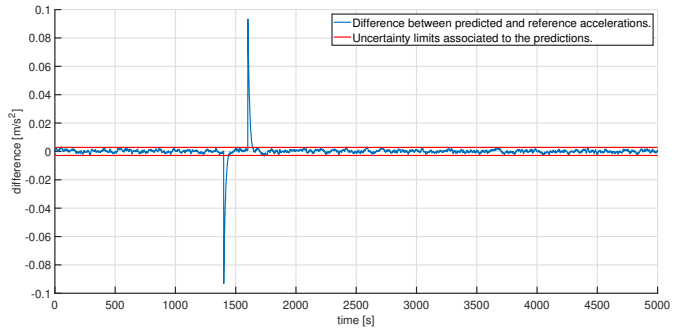

Fig. 16. Difference in the reference and predicted acceleration values (blue line) provided by the possibilistic Kalman filter defined in this paper, together with the predicted uncertainty interval (red lines).

coverage interval (red lines). The improvement, with respect to the implementation shown in Sect. III-C is, once again, the absence of oscillations.

It can be concluded that the defined possibilistic KF improves the behavior of the possibilistic Kalman filter defined in [16], since both predictions and uncertainty are correctly evaluated.

IV. Validation of the Proposed Possibilistic Kalman Filter

In order to validate the possibilistic Kalman filter defined in this paper, this section shows the results obtained by employing an hybrid KF, in which the variables are partly processed according to the theory of possibility, and partly according to the theory of probability. In particular, the random contributions to uncertainty have been processed according to the classical KF equations, while the systematic contributions to uncertainty have been modeled and processed as internal PDs of RFVs, by applying the RFV mathematics. In this way, the systematic contribuitions can be correctly propagated [1]–[3]. The algorithm in this case is schematically described in Fig. 17.

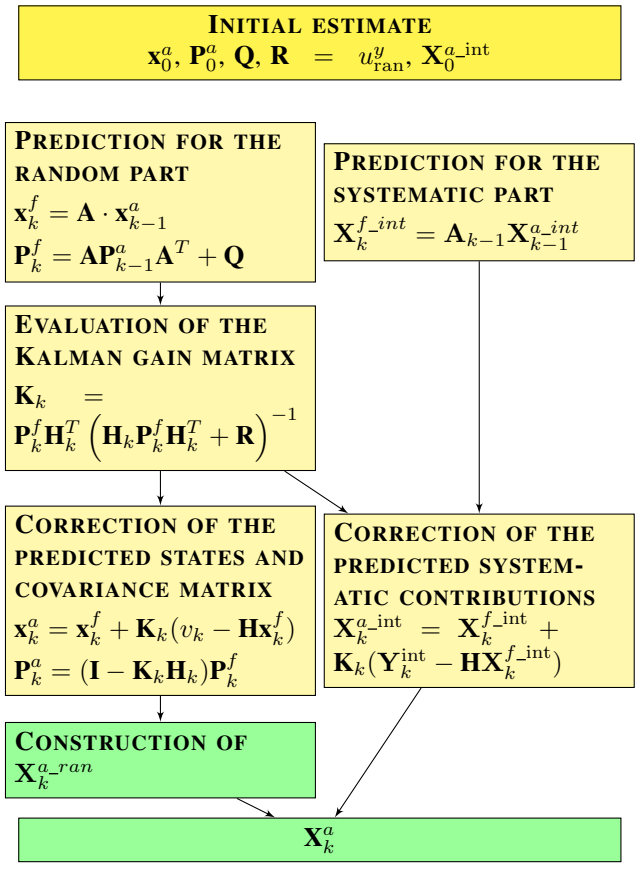

Fig. 17. The employed algorithm to validate the proposed possibilistic Kalman filter.

As far as the classical KF is concerned, the same assumptions are done as in Sect. III-A except that, in this case, the standard uncertainty associated to the simulated measured velocity is u_{ran}^v (and not u^v), since only the random

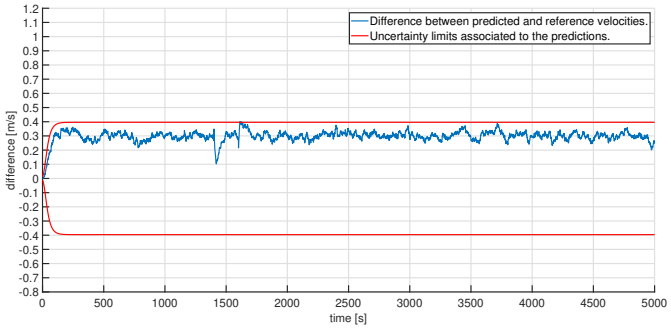

Fig. 18. Difference in the reference and predicted velocity values (blue line) provided by the hybrid Kalman filter, together with the predicted uncertainty interval (red lines).

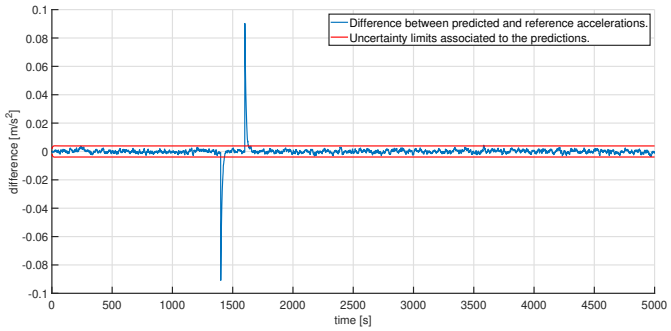

Fig. 19. Difference in the reference and predicted acceleration values (blue line) provided by the hybrid Kalman filter, together with the predicted uncertainty interval (red lines).

contributions are now considered. As for the RFV part, it is sufficient to consider only the initial internal PDs of velocity and acceleration in the initial state $\mathbf{X}_0^{a\_\text{int}}$, as defined in Sect. III-C.

The obtained results are shown in Figs. 18 and 19.

The blue line in Fig. 19 shows the differences between the reference and the predicted accelerations and the red line gives the evaluated uncertainty intervals.

The blue line in Fig. 18 represents the difference between the predicted velocity (directly provided by the classical KF, at the left side of the algorithm's model) and $v_{\text{ref}}(k)$. On the other hand, the red intervals represent, for every iteration, the 99% confidence interval of the RFV associated at the *a posteriori* velocity. In order to obtain this RFV, at every iteration, it is possible to combine the internal PD (obtained with the RFV mathematics, at the right side of the algorithm's model in Fig. 17) with the random PD built according to the results given by the classical KF at the same step (obtained by applying the probability-possibility transformation to the pdf given at the left side of the algorithm's model in Fig. 17). In particular, we obtain the random PD by applying the probability-possibility transformation [1] to the normal pdf whose mean value is the first element in $\mathbf{x}_k^a$ and whose standard deviation is given by the element $(1,1)$ in the covariance matrix $\mathbf{P}_k^a$.

In this case, we have convergence after about 85 iterations and the standard deviation of the blue line in the results is $30.8 \cdot 10^{-3}\text{m/s}$ after reaching convergence.

By comparing Fig. 15 with Fig. 18, it can be immediately seen that we have obtained very similar results, thus confirming the validity of the proposed possibilistic KF. Of course, the application of the possibilistic KF is much more immediate than the application of the Hybrid KF.

V. Further tests and comparison

In order to achieve a more comprehensive validation of the proposed possibilitic KF, the same simulations as those reported in Sect. III and IV have been repeated by considering the pattern shown in Fig. 20 for velocity and acceleration.

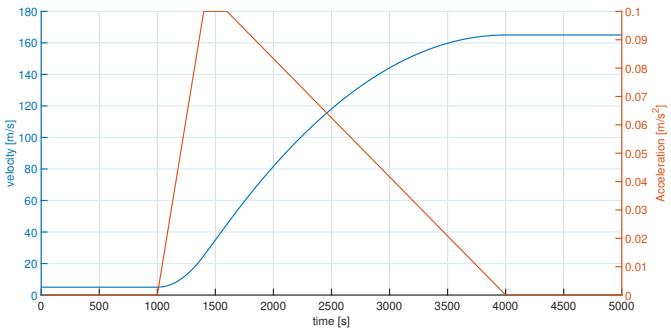

Fig. 20. Reference values of velocity (blue line) and acceleration (red line) over time for the new considered case.

The obtained results are quite similar to those reported in Figs. 6, 7, 9, 10, 12, 13, 15, 16, 18 and 19 and are not reported here for the sake of brevity.

Instead, more synthetic indexes have been extracted from the obtained results, for a more immediate comparison of the different considered KFs. In particular:

- Conversion time. It is the time taken to reach the 90% of the steady-state value of the prediction.
- Steady-state error. It is the difference between the average predicted value and the reference value, once steady state is reached.
- Error variation. It is the standard deviation of the error once steady state is reached.
- Uncertainty limits. It is the width of the coverage interval that is supposed to encompass the error on the predicted value with a 99% coverage probability, once steady-state is reached. When the classical KF is employed, this is the $\pm 1.96\sigma$ interval. When the possibilistic KF is employed, this is the width of the α-cut at $\alpha = 0.01$ level of the RFV of the predicted values.
- Variation of uncertainty limits. It is the standard deviation of the width of the interval considered above, for the predicted values, once steady state is reached.
- Percentage of values inside the uncertainty limits. It is the relative number of predicted values whose error falls inside the above interval. This value should be, theoretically, 99%. The closer it approximates this value, the more accurate is the prediction provided by the considered KF.

All above indexes have been computed and reported in Table I (velocity) and Table II (acceleration) for the simulated pattern shown in Fig. 3, and in Table III (velocity) and Table IV (acceleration) for the simulated pattern shown in Fig. 20.

KF	Classical	Schmitt	Original Possibilistic	Modified Possibilistic	Hybrid
Convergence(s)	54	847	117	151	85
Steady-state error	0.2961	0.2968	0.3016	0.3024	0.2997
Variation of error	0.0299	0.0267	0.0847	0.0224	0.0308
Uncertainty limits	± 0.0371	± 0.1871	± 0.4056	± 0.3706	± 0.3961
Variation of uncertainty limits	0	0	0.0656	0	0
Percentage inside the uncertainty limits	0.34	5.14	82.36	97.38	99.92

TABLE I
SYNTHETIC INDEXES FOR VELOCITY FOR CASE 1 AS SEEN IN FIG. 3.

KF	Classical	Schmitt	Original Possibilistic	Modified Possibilistic	Hybrid
Convergence(s)	10	10	3	7	9
Steady-state error	-0.00009	0.00003	0.00052	0.00002	-0.00007
Variation of error	0.0012	0.0011	0.00086	0.00084	0.0011
Uncertainty limits	± 0.0015	± 0.0015	± 0.0018	± 0.0028	± 0.0039
Variation of uncertainty limits	0	0	0	0	0
Percentage inside the uncertainty limits	81.14	83.70	93.88	98.42	98.72

TABLE II
SYNTHETIC INDEXES FOR ACCELERATION FOR CASE 1 AS SEEN IN FIG. 3.

KF	Classical	Schmitt	Original Possibilistic	Modified Possibilistic	Hybrid
Convergence(s)	54	847	117	151	85
Steady-state error	0.2969	0.3138	0.2913	0.3036	0.3032
Variation of error	0.0251	0.0316	0.0843	0.0276	0.0287
Uncertainty limits	± 0.0371	± 0.1871	± 0.4056	± 0.3706	± 0.3961
Variation of uncertainty limits	0	0	0.0656	0	0
Percentage inside the uncertainty limits	0.2	11.96	83.10	99.76	99.88

TABLE III
SYNTHETIC INDEXES VELOCITY FOR CASE 2 AS SEEN IN FIG. 20.

KF	Classical	Schmitt	Original Possibilistic	Modified Possibilistic	Hybrid
Convergence(s)	10	10	3	7	9
Steady-state error	0.000075	0.0020	0.00062	0.00012	0.00028
Variation of error	0.0011	0.0024	0.0018	0.00096	0.0010
Uncertainty limits	± 0.0015	± 0.0015	± 0.0010	± 0.0028	± 0.0039
Variation of uncertainty limits	0	0	0	0	0
Percentage inside the uncertainty limits	79.40	37.72	77.88	95.96	99.18

TABLE IV
SYNTHETIC INDEXES FOR ACCELERATION FOR CASE 2 AS SEEN IN FIG. 20.

The reported data confirm that the proposed possibilistic KF provides good results in the presence of systematic contributions to uncertainty and that the hybrid KF can be considered as a reference method.

VI. CONCLUSIONS

This paper defines a possibilistic KF, which is an improvement of the one defined in [16].

By considering a simple example, the results obtained by applying the proposed possibilistic KF are shown and compared with the results obtained by applying the classical KF, the Schmidt KF and the possibilistic KF defined in [16] to the same example.

The obtained results show that the proposed possibilistic KF provides better results than the other available considered methods for implementing a KF in the presence of systematic errors. In fact, the classical and Schmidt KF fail in evaluating uncertainty when a systematic error is present, while the possibilistic KF proposed in [16] provides a good evaluation of uncertainty but is very noisy in predicting the state variables. On the other hand, the proposed possibilistic KF provides a smooth prediction of both the state variables and uncertainty.

The validity of the proposed possibilistic KF is proved by considering an hybrid KF which combines the classical KF (in taking into account the random uncertainty contributions) and RFV mathematics (for taking into account the systematic uncertainty contributions). The obtained results are very similar to the ones obtained with the proposed possibilistic KF, thus showing the correctness of the proposed approach.

Even if these two last simulations provide very similar results, it is evident the advantage in the use of the proposed possibilistic KF, since the algorithm is simpler and a unique mathematical approach is followed.

In conclusion, the possibilistic version of the KF proposed

here appears to be quite promising in all applications when systematic contributions to uncertainty cannot be neglected. This may include model bias and the effect of uncompensated influence quantities (such as, for instance, temperature) on the values provided by the sensors. Even if the classical KF is still capable of providing a good prediction of the state variables, the proposed possibilistic KF can also provide a good prediction of uncertainty that, in measurement applications, is as important as the predicted value of the state variable. Indeed, measured values without uncertainty cannot be considered valid measurement results.

REFERENCES

[1] S. Salicone and M. Prioli. *Measurement Uncertainty within the Theory of Evidence*. Springer series in Measurement Science and Technology. Springer, New York, NY, USA, 2018.

[2] A. Ferrero and S. Salicone. A comparison between the probabilistic and possibilistic approaches: The importance of a correct metrological information. *IEEE Trans. Instrum. Meas.*, 67(3):607–620, March 2018.

[3] A. Ferrero and S. Salicone. Uncertainty: Only one mathematical approach to its evaluation and expression? *IEEE Trans. Instrum. Meas.*, 61(8):2167–2178, 2012.

[4] G. Mauris, V. Lasserre, and L. Foulloy. A fuzzy approach for the expression of uncertainty in measurement. *Measurement*, 29:165–177, 2001.

[5] G. Mauris, L. Berrah, L. Foulloy, and A. Haurat. Fuzzy handling of measurement errors in instrumentation. *IEEE Trans. Instrum. Meas.*, 49(1):89–93, 2000.

[6] M. Urbanski and J. Wasowsky. Fuzzy approach to the theory of measurement inexactness. *Measurement, Elsevier Science*, 34:67–74, 2003.

[7] A. Ferrero and S. Salicone. The random-fuzzy variables: a new approach for the expression of uncertainty in measurement. *IEEE Trans. Instrum. Meas.*, 53(5):1370–1377, 2004.

[8] Q. Zhu, Z. Jiang, Z. Zhao, and H. Wang. Uncertainty estimation in measurement of micromechanical properties using random-fuzzy variables. *Review of Scientific Instruments*, 77(035107), 2006.

[9] M. Pertile, M. De Cecco, and L. Baglivo. Uncertainty evaluation in two-dimensional indirect measurement by evidence and probability theories. *IEEE Trans. Instrum. Meas.*, 59(11):2816–2824, 2010.

[10] M. Pertile and M. De Cecco. Uncertainty evaluation for complex propagation models by means of the theory of evidence. *MEASUREMENT SCIENCE AND TECHNOLOGY*, 19:1–10, 2008.

[11] Chin Wang Lou and Ming Chui Dong. A novel random fuzzy neural networks for tackling uncertainties of electric load forecasting. *Electrical Power and Energy Systems*, 73:34–44, 2015.

[12] Yan Tu, Xiaoyang Zhou, Jun Gang, Merrill Liechty, Jiuping Xu, and Benjamin Lev. Administrative and market-based allocation mechanism for regional water resources planning. *Resources, Conservation and Recycling*, 95:156?73, 2015.

[13] Dongping Chen, Xuening Chu, Xiwu Sun, and Yupeng Li. A new product service system concept evaluation approach based on information axiom in a fuzzy-stochastic environment. *International Journal of Computer Integrated Manufacturing*, 28(11):1–19, 2015.

[14] R. Faragher. Understanding the basis of the kalman filter via a simple and intuitive derivation. *IEEE Signal Processing Magazine*, 29(5):128–132, September 2012.

[15] Roman Y Novoselov, Shawn M Herman, Sabino M Gadaleta, and Aubrey B Poore. Mitigating the effects of residual biases with schmidt-kalman filtering. In *2005 7th International Conference on Information Fusion*, volume 1, pages 8–pp. IEEE, 2005.

[16] A. Ferrero, R. Ferrero, S. Salicone, and W. Jiang. The kalman filter uncertainty concept in the possibility domain. *IEEE Trans. Instrum. Meas.*, 68(11):4335–4347, November 2019.

[17] W. Wei, S. Gao, Y. Zhong, C. Gu, and A. Subic. Random weighting estimation for systematic error of observation model in dynamic vehicle navigation. *International Journal of Control, Automation and Systems*, 14(2):514–523, April 2016.

[18] Y. Yang, N. Rees, and T. Chuter. Reduction of encoder measurement errors in ukirt telescope control system using a kalman filter. *IEEE Transactions on Control Systems Technology*, 10(1):149–157, Jan 2002.

[19] B. Noack, V. Klumpp, and U. D. Hanebeck. State estimation with sets of densities considering stochastic and systematic errors. In 12^{th} *International Conference on Information Fusion*, Seattle, WA, USA, July 6-9, 2009.

[20] F. Matìa, A. Jiménez, B. M. Al-Hadithi, D. Rodrìguez-Losada, and R. Galán. The fuzzy kalman filter: State estimation using possibilistic techniques. *Fuzzy Sets and Systems*, 157(16):2145 – 2170, 2006.

[21] M. Oussalah and J. De Schutter. Possibilistic kalman filtering for radar 2d tracking. *Information Sciences*, 130(1):85 – 107, 2000.

[22] JCGM 100:2008. *Evaluation of Measurement Data – Guide to the Expression of Uncertainty in Measurement, (GUM 1995 with minor corrections)*. Joint Committee for Guides in Metrology, 2008.

[23] JCGM 200:2012. *International Vocabulary of Metrology – Basic and General Concepts and Associated Terms (VIM 2008 with minor corrections)*. Joint Committee for Guides in Metrology, 2012.

[24] G. Shafer. *A Mathematical Theory of Evidence*. Princeton Univ. Press, Princeton, NJ, USA, 1976.

[25] A. Ferrero and S. Salicone. The construction of random-fuzzy variables from the available relevant metrological information. *IEEE Trans. Instrum. Meas.*, 58(2):1149–1157, 2009.

[26] S. Salicone. *Measurement Uncertainty: an approach via the mathematical theory of evidence*. Springer series in reliability engineering. Springer, New York, NY, USA, 2007.

[27] A. Ferrero, M. Prioli, S. Salicone, and B. Vantaggi. 2D probability-possibility transformations. In *Synergies of Soft Computing and Statistics for Intelligent Data Analysis*, volume 190 of *Advances in Intelligent Systems and Computing*, pages 63–72. Springer Berlin Heidelberg, 2013.

[28] https://www.gps.gov/systems/gps/performance/accuracy/.

[29] A. Ferrero, M. Prioli, and S. Salicone. Joint random-fuzzy variables: A tool for propagating uncertainty through nonlinear measurement functions. *IEEE Trans. Instrum. Meas.*, 65(5):1015–1021, May 2016.